International Conference on Case Histories in Geotechnical Engineering

(2008) - Sixth International Conference on Case Histories in Geotechnical Engineering

16 Aug 2008, 8:45am - 12:30pm

Seismic Response of Structures with Underground Stories Considering Non-Linear Soil-Structure Interaction

Amir H. Halabian
Isfahan University of Technology, Isfahan, Iran

S. Hamid Hashemolhosseini
Isfahan University of Technology, Isfahan, Iran

Hessam Saldourgar
Isfahan University of Technology, Isfahan, Iran

SEISMIC RESPONSE OF STRUCTURES WITH UNDERGROUND STORIES CONSIDERING NON-LINEAR SOIL-STRUCTURE INTERACTION

Amir M. Halabian
Faculty of Civil Engineering
Isfahan University of Technology
Isfahan, Iran

S. Hamid Hashemolhosseini
Faculty of Mining Engineering
Isfahan University of technology
Isfahan, Iran

Hessam Saldourgar
Faculty of Civil Engineering
Isfahan University of technology
Isfahan, Iran

ABSTRACT

Most of the research conducted for soil-structure interaction analysis of structures are assuming the linear behavior of soil. It is well known that during strong ground excitations the soil adjacent to the structure behaves highly non-linear. The nonlinear soil behavior affects the soil-structure interaction in a complex way especially because of the inadequacy in modeling the unbounded soil medium. In the case where an elastic soil behavior is assumed, the surface motion will be amplified proportionally to the input motion. However, in reality the amplitude and frequency content of the response are modified due to the soil's stiffness degradation and higher energy dissipation. The present work deals with the influence of soil non-linearity, introduced by hysteretic behavior of near-field soil, on the soil-foundation-structure interaction phenomena. The objective is to reveal the beneficial or detrimental effects of the non-linear SSI concerning both the drift and settlement of structures with underground stories. To examine the effect of non-linear soil-structure interaction a realistic non-linear soil model is incorporated into the finite difference FLAC software. To better understanding the non-linear dynamic SSI, interface elements are also used between the near-field soil and basement walls. For a practical structure throughout a parametric study, some non-linear seismic analyses are performed to demonstrate the effectiveness of the affecting parameters in response of the structure. The results showed much difference on seismic response of structure such as drift, settlement and developing pressure around the basement walls when the non-linear soil-structure interaction is considered.

INTRODUCTION

The soil-structure interaction (*SSI*) is a complicated phenomenon for structures coupled with the soil medium, which is generally semi-infinite in extent and non-linear in its material behavior. The problem of *SSI* in the seismic analysis of high-rise buildings with underground stories has become increasingly important, as it may be inevitable to build such a structures for the sites with less-favorable geotechnical conditions due to ever-increasing difficulty in acquiring new construction sites. Most of the research conducted for soil-structure interaction analysis of structures are assuming the linear behavior of soil. However, it is well understood that during strong ground excitations the soil adjacent to the structure behaves highly non-linear. The nonlinear soil behavior affects the soil-structure interaction in a complex way especially because of the inadequacy in modeling the unbounded soil medium. This phenomenon could greatly contribute to the response of supported structures to seismic loading, and in some cases it may become the governing factor when choosing a retrofitting scheme. The seismic response of buildings with basement walls is a complicated phenomenon and is affected by several factors including non-linear soil-structure interaction.

Interaction problems in dynamic structural analysis involve the determination of the response of a structure placed in an unbounded soil subjected to a transient load. Any analysis of dynamic SSI can be performed using two rigorous numerical methods: the direct method and substructure method. The direct method is conceptionally the easiest rigorous way to account for *SSI* in the seismic analysis of structures. In this method, the structure and semi-infinite unbounded soil zone supporting the structure may be modeled by any numerical method such as finite-element method. Using direct method, the effect of surrounding unbounded soil can be approximately taken into account by imposing transmitting boundaries along a fictitious interface enclosing the soil-structure system where the free-field motion is also applied. The response of structure can be calculated with acceptable accuracy by placing artificial boundaries sufficiently far away from the structure-medium interface.

Alternatively, the soil environment may be treated as mixed boundary value and initial value conditions, and then the soil-structure system is broken into two distinct parts, superstructure and substructure. These subsystems are connected by the general soil-structure interface. The superposition inherent to this approach, so-called substructure method, assumes linear soil behavior. The dynamic analysis of the superstructure is performed using the impedance functions of the substructure. The modification of the input seismic motion, which results from the actual interaction when superstructure is inserted into seismic environment of the free field, is evaluated. Because the principle of superposition is assumed in the analysis, the substructure approach is limited to linear or equivalent linear problems. Therefore, the unbounded soil is assumed to be linear but the superstructure could be assumed linear or non-linear.

Accordingly, the direct method is the most suitable approach to take into account the effect of soil cyclic nonlinear behavior on the soil-structure interaction phenomena. Knowing this fact that implementing advanced constitutive models into the direct numerical analysis method requires remarkable computational efforts, a simple algorithm to define the soil hysteretic loops during loading-reloading phase of excitation is employed. In this study, the elastic behavior of supporting soil in the soil-structure system is assumed to show the hysteretic characteristics based on the hyperbolic model for stress-strain relationships. Therefore, the cyclic non-linear behavior for the soil unbounded medium is accounted either for free-field analysis or inertial analysis. The Finite difference method is used to solve the governing dynamic equations of a soil-structure system. To take into account the consistency between the dynamic properties of the supporting soil and the frequency content of the excitation, the material properties of the supporting soil are selected so that the natural frequency of the stratum is compatible with the predominant frequency of the ground motion.

The numerical procedure proposed in this study is implemented to examine the effect of soil non-linearities on the dynamic soil-structure analysis of a practical five-story building supported by a shallow foundation subjected to some selected strong ground motions. For a given excitation, appropriate site parameters are chosen to enforce the inelastic behavior of the soil. The role of several parameters on both the structural response and base displacements are extensively studied. This parametric study concerns the different soil properties as well as the characteristics of the input motion.

NONLINEAR DIRECT APPROACH

The non-linear dynamic analysis of soil-structure systems can be classified into the equivalent linear and the nonlinear approaches. In the equivalent-linear method, a linear analysis is performed, with some initial values assumed for damping ratios and shear modulus in the various regions of the model. Then, the maximum shear strain is computed for each element and used to determine new values for damping and shear modulus of elasticity, by reference to laboratory-derived curves that relate damping ratio and secant shear modulus of elasticity to amplitude of dynamic shear strain. These new values of damping ratio and shear modulus are then used in a new linear analysis of the model. The whole process is repeated several times, until there are no further changes in properties. It is said that converging points are representative of the response of the real site.

In contrast, non-linearity introduced by the constitutive behavior of soil leads the governing dynamic equilibrium equations to be reduced to the incremental form. Therefore, only one run is done with a fully nonlinear method, since non-linearity in the stress-strain law is followed directly by each element. Provided that an appropriate law is used, the dependence of damping and shear modulus on strain level are automatically modeled.

Both methods have their advantages and disadvantages. In the equivalent linear method, for each element constant linear properties estimated from the mean level of dynamic motion are used. The disadvantages of the method are that the method does not directly provide information on irreversible deformations. Also plastic yielding is modeled inappropriately and the interface and mixing phenomena that occur between different frequency components in a nonlinear material are missing from an equivalent linear analysis. On the other hand equivalent linear method takes much more liberties with physics, user friendly and accepts laboratory results from cyclic tests directly. On the other hand, using non-linear material law into a general non-linear analysis approach makes interference and mixing of different frequency components occur naturally. Besides, irreversible displacements and other permanent changes are also modeled automatically and a proper plasticity formulation can be used. Employing this method, the use of different constitutive models may be studied easily, while the approach needs more computationally efforts.

An accurate non-linear dynamic soil-structure interaction problem requires an efficient solving algorithm as well as a nonlinear soil constitutive law that also captures the hysteretic behavior of soil during loading and reloading phases of transient loads to represents energy-absorbing characteristics of soil material. FLAC 3D (Itasca Consulting Group, 1996) is a numerical computer widely used in geotechnical engineering based on explicit finite difference scheme. The non-linear soil model adapted in the program can correctly represent the physics of the real soil; however, it needs more parameters to define the soil behavior resulting not being user friendly from structural engineer's point of view. If hysteretic-type model is used and no extra damping is specified, then the damping and tangent modulus are appropriate to the level of excitation at each point in time and space, since these parameters are embodied in the constitutive model. In this study, the elastic behavior of soil in the model ground is assumed to show the hysteretic characteristics based on the hyperbolic model for stress-strain relationships. Fig. 1 shows the typical hysteretic curve on the τ-γ relationships (Ishihara, 1998). The skeleton curve is given by the following hyperbolic equation:

$$\tau = \frac{G_0}{1+\gamma / \gamma_r}\gamma \tag{1}$$

As seen in Fig. 1, G_0 is the shear modulus at the initial part of the backbone curve and γ_r is the reference strain defined as

$$\gamma_r = \frac{\tau_f}{G_0} \tag{2}$$

where τ_f is the soil shear strength (horizontal asymptote at large strains) and τ and γ are given as follows:

$$\tau = \sigma_1 - \sigma_3 \quad ; \quad \gamma = \varepsilon_1 - \varepsilon_3 \tag{3}$$

G_0 can be obtained by Hardin-Dernevich relation (Prakash 1981):

$$G_0 = \alpha \frac{(2.973-e)^2}{1+e} . (\frac{1+2k_0}{3})^{1/2} . \sqrt{\sigma'_v} \tag{4}$$

in which e , σ'_v , K_0 and are void ratio, effective vertical stress and confining pressure ratio, respectively.

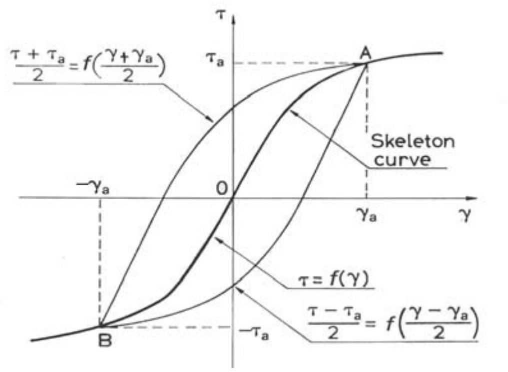

Fig. 1. Soil stress-strain relationship

The sign of the γ increment, $d\gamma$, judges the reversal of loading direction. For each loading-reloading loop, after reversal point, the unloading path is defined as

$$\frac{\tau - \tau_a}{2} = f\left(\frac{\gamma - \gamma_a}{2}\right) \tag{5}$$

in which τ_a and γ_a are the shear stress and shear strain at the reversal point. In the hyperbolic model the tangent shear modulus of elasticity for loading and reloading can be obtained from:

$$G_t = \begin{cases} \dfrac{G_{\max}}{\left[1-\left(G_{\max}/\tau_{\max}\right)|\gamma|\right]^2} & \textit{for loading} \\ \dfrac{G_{\max}}{\left[1-\left(G_{\max}/2\tau_{\max}\right)|\gamma-\gamma_\varepsilon|\right]^2} & \textit{for reloading} \end{cases} \tag{6}$$

In this study, an energy dissipation approach was used to predict the reversal point in loading-reloading paths of hysteretic loop. Based on this approach the reversal loading direction is judged by the sign of the dissipated energy increment (the incremental shear work), ΔW_S. The shear work increment can be obtained in a FEM analysis as the different between the total incremental work, ΔW_T, and the incremental volumetric work, ΔW_N, for an increment strain during loading or reloading as

$$\Delta W_s = \Delta W_T - \Delta W_N \tag{7}$$

where

$$\Delta W_T = \sigma_{11}\Delta\varepsilon_{11} + \sigma_{22}\Delta\varepsilon_{22} + \sigma_{33}\Delta\varepsilon_{33} + 2(\sigma_{12}\Delta\varepsilon_{12} + \sigma_{13}\Delta\varepsilon_{13} + \sigma_{23}\Delta\varepsilon_{23})$$

(8)

$$\Delta W_N = 1/3 . \sum_{k=1}^{k=3} \sigma_{kk}\Delta\varepsilon_{kk} \tag{9}$$

The rebound shear modulus can be calculated by effective stresses through a non-linear dynamic analysis. This basic model can produce curves of apparent damping and modulus versus cyclic strain that resemble results from laboratory tests (Fig. 2).

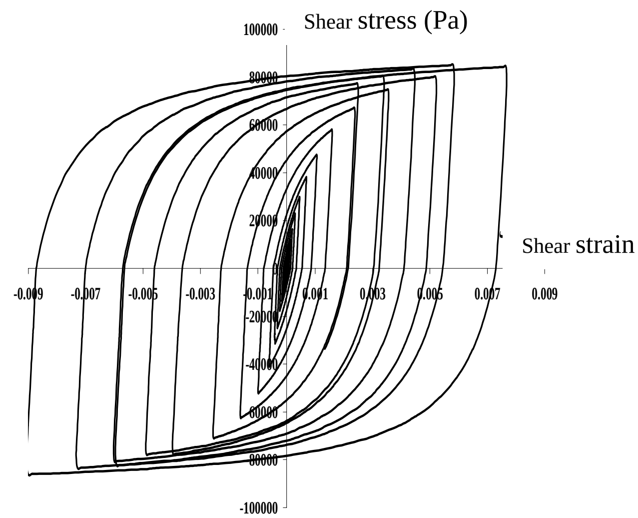

Fig. 2. Cyclic shear stress-shear strain curve for an element in FE model

In the plastic zone the Mohr-Coulomb failure constitutive model was adopted where the failure envelope corresponds to Mohr-Coulomb criteria. According to this theory, failure along a plane in the soil occurs by a critical combination of normal and shear stresses and not by normal or shear stress alone. The functional relation between normal and shear stress on the failure, generally referred to as the Mohr-Coulomb criteria, can be given by a failure envelope defined as

$$\tau_f = c' + \sigma'_{nf} \tan\varphi' \tag{10}$$

where τ_f and σ'_{nf} are the shear and normal effective stresses on the failure plane, c' is cohesion and φ' is the drained angle of shearing resistance.

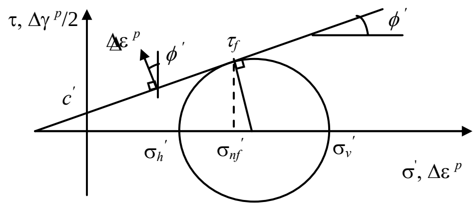

Fig.3. Failure envelope

The criterion may be represented in the plane (σ'_1, σ'_3), defining the failure criterion as

$$\sigma'_1 - \sigma'_3 = 2c'\cos\varphi' + \left(\sigma'_1 + \sigma'_3\right)\sin\varphi' \tag{11}$$

The Mohr-Coulomb is assumed to be perfectly plastic, therefore, there is no hardening/softening criteria required (Fig. 4a). Using the Mohr-Coulomb criteria, the yield function can be defined as:

$$F\left(\{\sigma'\},\ \{k\}\right) = \sigma'_1 - \sigma'_3 - 2c'\cos\varphi' + \left(\sigma'_1 + \sigma'_3\right)\sin\varphi' \tag{12}$$

This function separates the elastic from elasto-plastic behaviors. It can be noted that the surface is a function of the stress state, $\{\sigma'\}$, and changes as a function of state parameters, $\{k\}$, which can be related to hardening or softening parameters. The state parameter $\{k\} = \{c', \varphi'\}^T$ is independent of plastic strain.

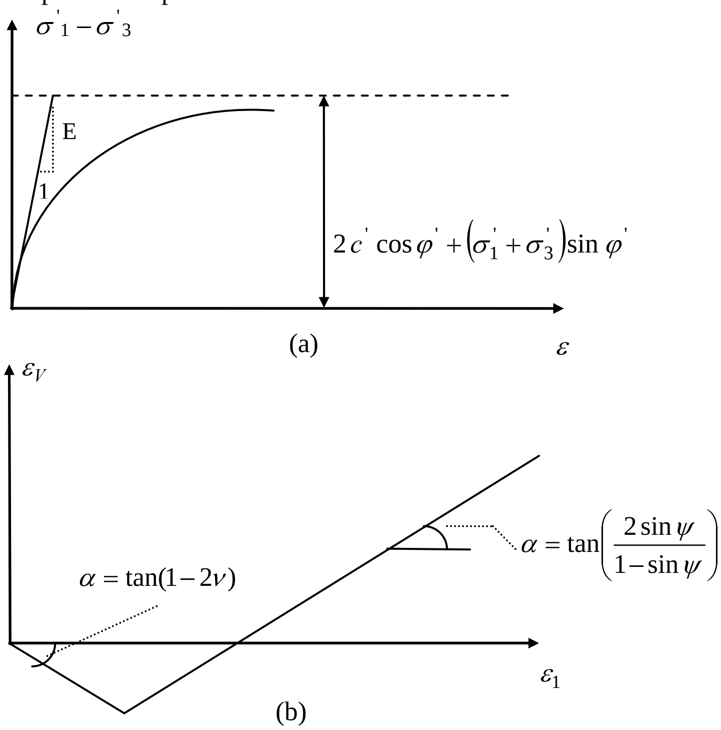

Fig. 4. Mohr-Coulomb elasto-plastic constitutive relationship

Using this Mohr-Coulomb criterion, Mohr-Coulomb constitutive model can be constructed where the failure envelope for this model corresponds to Mohr-Coulomb criterion (shear yield function) with cutoff (tension yield function). The position of stress point on this envelope is controlled by a non-associated rule for shear failure and an associated rule for tension failure. In the tension failure, the plastic strain increment vector is inclined at angle ϕ' to the vertical (Fig. 3) turning in a dilative plastic volumetric strain (Fig. 4b). The angle of dilation, ψ, defined by

$$\psi = \sin^{-1}\left(-\frac{\Delta\varepsilon_1^p + \Delta\varepsilon_3^p}{\Delta\varepsilon_1^p - \Delta\varepsilon_3^p}\right) \tag{13}$$

in which $\Delta\varepsilon_1{}^p$ and $\Delta\varepsilon_2{}^p$ are the principal plastic strain increments. In summary, in the Mohr-Coulomb model, c', φ' and ψ control the plastic behavior, while E and ν control the elastic behavior. If associated conditions are assumed, the number of model parameter reduces to 4 as $\psi = \varphi'$.

If c' and φ' are assumed large enough, the soil shear strength would be much larger than the induced soil stresses during the cyclic loading; therefore the soil will not experience the plastic deformation (Fig. 2). In the absence of large failure shear stress, the cyclic behavior of soil is controlled by both elastic and plastic behavior represented by Mohr-Coulomb elasto-plastic model (Fig.5).

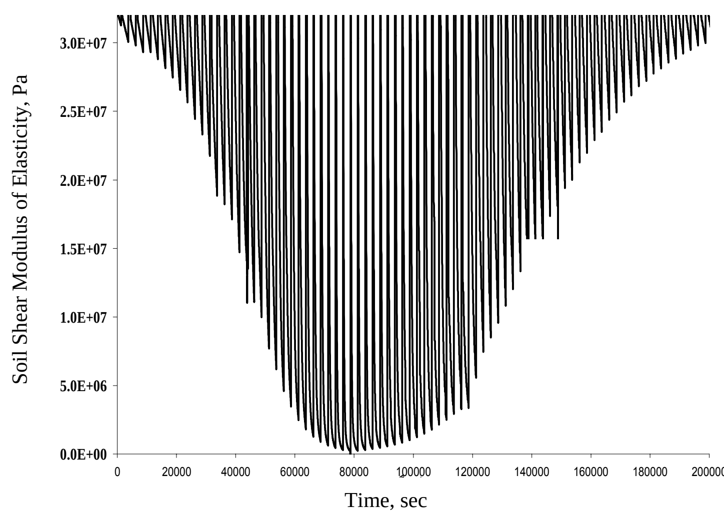

Fig. 5 Variation of soil shear modulus of elasticity during the loading

SOIL-STRUCTURE MODELING

If only the seismic excitation is considered, the equations of motion of a total structure-soil system (Fig. 6) can be written as

$$\begin{bmatrix} \mathbf{M}_{SS} & \mathbf{0} & \mathbf{0} \\ \mathbf{0} & \mathbf{M}_{II} & \mathbf{0} \\ \mathbf{0} & \mathbf{0} & \mathbf{M}_{FF} \end{bmatrix} \begin{Bmatrix} \ddot{\mathbf{u}}_s \\ \ddot{\mathbf{u}}_I \\ \ddot{\mathbf{u}}_F \end{Bmatrix} + \begin{bmatrix} \mathbf{C}_{SS} & \mathbf{C}_{SI} & \mathbf{0} \\ \mathbf{C}_{IS} & \mathbf{C}_{II} & \mathbf{C}_{IF} \\ \mathbf{0} & \mathbf{C}_{FI} & \mathbf{C}_{FF} \end{bmatrix} \begin{Bmatrix} \dot{\mathbf{u}}_S \\ \dot{\mathbf{u}}_I \\ \dot{\mathbf{u}}_F \end{Bmatrix} + \begin{bmatrix} \mathbf{K}_{SS} & \mathbf{K}_{SI} & \mathbf{0} \\ \mathbf{K}_{IS} & \mathbf{K}_{II} & \mathbf{K}_{IF} \\ \mathbf{0} & \mathbf{K}_{FI} & \mathbf{K}_{FF} \end{bmatrix} \begin{Bmatrix} \mathbf{u}_S \\ \mathbf{u}_I \\ \mathbf{u}_F \end{Bmatrix} = \begin{Bmatrix} 0 \\ \mathbf{R}_i(t) \end{Bmatrix} \quad (14)$$

in which $\mathbf{u}^t$ is the total displacement vector; **M**, **C** and **K** are the mass, damping and stiffness matrices obtained by the finite-element formulation for the structure and for the substructure soil in the *SS* system. The subscript "*s*" denotes

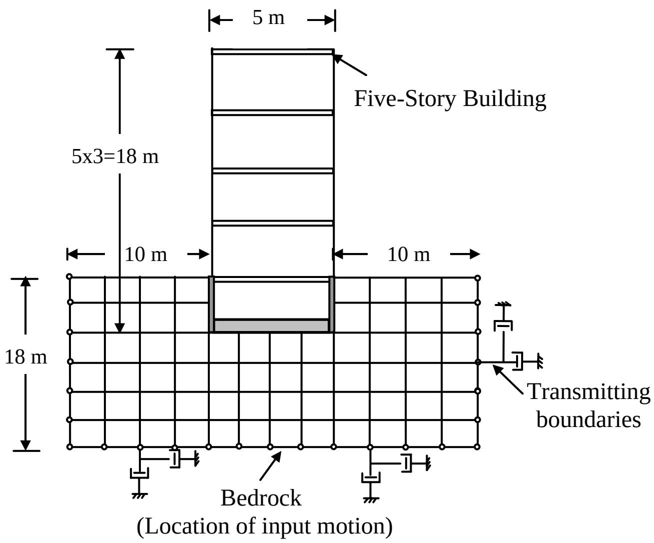

Fig. 6. Soil-Structure system

the degrees of freedom in the superstructure of *SS* system; the subscript "*I*" represents those along the structure-soil interface between the superstructure and substructure; the bounded soil zone (substructure) is represented by superscript "*F*"; and $\mathbf{R}_i(t)$ is the earthquake force applied along the general structure-soil interface, which can be calculated from the free-field responses, $\ddot{\mathbf{u}}_g$, as

$$\mathbf{R}_i(t) = -\begin{bmatrix} \mathbf{M}_{SS} & \mathbf{0} & \mathbf{0} \\ \mathbf{0} & \mathbf{M}_{II} & \mathbf{0} \\ \mathbf{0} & \mathbf{0} & \mathbf{M}_{FF} \end{bmatrix} \mathbf{I}\, \ddot{\mathbf{u}}_g \quad (15)$$

where $\ddot{\mathbf{u}}_g$ is the input ground motion applied to the bedrock which is evaluated using free-field analysis, and **I** is the unity vector.

GROUND ACCELERATION MOTION

The ground motion at the bedrock, called system input motion, $\ddot{u}_g$, can be calculated from the free-field analysis. Practically, for the purpose of the free-field analysis, it is assumed that the soil medium is a horizontally layered half space, and the seismic waves are generated by vertically incident plane body

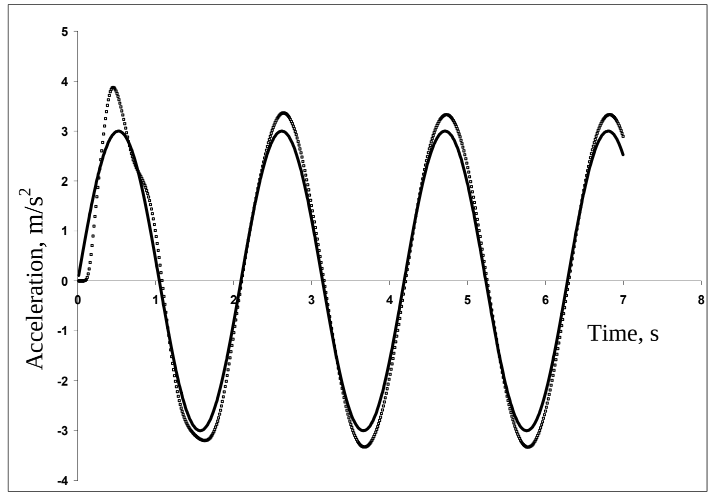

Fig. 7. Free field acceleration due to harmonic excitation for linear system

waves in the underlying half space, which are implemented into the computer program SHAKE 91. The dynamic equilibrium equations for horizontal layers can be obtained from the displacement and traction vectors at the interfaces of each layer based on analytical solutions for the plane body wave motion as

$$K_{(m)}(\omega) \begin{Bmatrix} u_{(m-1)}(\omega) \\ u_{(m)}(\omega) \end{Bmatrix} = \begin{Bmatrix} f_{(m-1)}(\omega) \\ f_{(m)}(\omega) \end{Bmatrix} \quad m = 1,2,....,n-1 \quad (16)$$

and for the underlying half space (if exists) as

$$K_n(\omega)\, u_{(n-1)}(\omega) = f_{(n-1)}(\omega) \quad (17)$$

in which $u_{(m)}$ and $f_{(m)}$ are the displacement and traction vectors on the upper interface of the m^{th} layer; $K_{(m)}$ is the frequency dependent dynamic stiffness matrix of the m^{th} layer, and n is the number of layers including the underlying half space. Therefore, given a control motion on any layer interface, the motions on the other layer interfaces can be computed by solving these equations successively. In general, the non-linear behavior is observed in the free-field motion due to the effect of wave scattering during the earthquake events. Hence, in the earthquake response analysis, this primary non-linear behavior shall be more carefully considered in the free-field ground motion. SHAKE 91 uses the equivalent linear analysis method to take into account the effect of primary non-linear behavior of soil. To demonstrate the effect of primary soil non-linear behavior on the free-field response, a homogeneous soil layer of thickness 18m assuming linear and non-linear behavior is considered to support the structure (Fig. 8). Two different excitations at the bedrock are considered to examine the effect of frequency content of the motion along with the type of supporting soil on the site's free-field responses. Table 1 shows the different soil parameters for each excitation, which are chosen to enforce the inelastic behavior of the soil. A harmonic acceleration with maximum amplitude of 0.3g is selected as the excitation applied to the bedrock. Fig. 7 shows the free-field response evaluated by FLAC3D when the soil behaves linearly. As it can be noted the peak ground acceleration for the free-field response has been amplified, while its frequency content is the same as the input motion. However, when the soil undergoes to the non-linear zone, the maximum acceleration of the free-field response is attenuated and the frequency content of the response is also altered (Fig. 8).

As another example of free-field analysis, the N-S corrected component of the 1940 El-Centro earthquake ground motion is applied to the bedrock. The soil later properties are chosen to enforce the inelastic behavior of the soil. Assuming the soil linear and non-linear behavior, the free-field motion is calculated using FLAC3D equipped by the strain dependent cyclic constitutive law described in this paper and also program SHAKE 91. Fig. 9 shows the free-field response of the soil stratum neglecting the primary soil non-linearity obtained from FLAC3D and SHAKE 91. While demonstrating an amplification to the free-field response compared the input motion, the excellent match can be observed between two programs. The free-field responses of the soil assuming non-linear behavior are shown in Figs. 10 and 11 obtained from dynamic non-linear analysis and equivalent linear analysis, respectively. It can be noted that the results are similar in terms of the acceleration amplitude, but different for the local frequency contents. It also shows that in the earthquake response analysis, the primary non-linear behavior shall be more carefully considered in the supporting soil associated to the free-field ground motion.

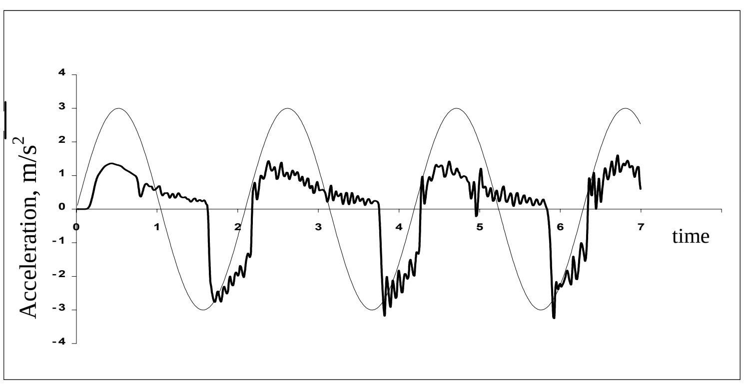

Fig. 8. Free field acceleration due to harmonic excitation for non-linear system

EXAMPLE CALCULATIONS

To investigate the effect of hysteretic behavior of soil on seismic response of structures with underground stories a practical five-story building supported by a shallow foundation subjected to two different ground motions was assumed. An ensemble of two strong ground motion records, the N-S component of the 1940 El Centro earthquake and Tarzana Station of the 1994 Northridge earthquake are

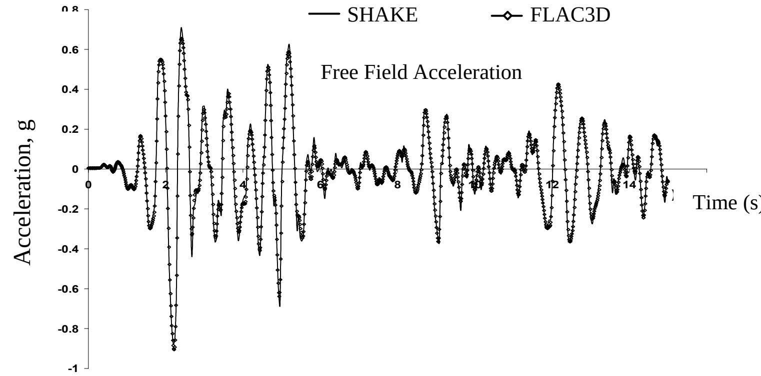

Fig. 9. Free field acceleration due to El Centro excitation for linear system

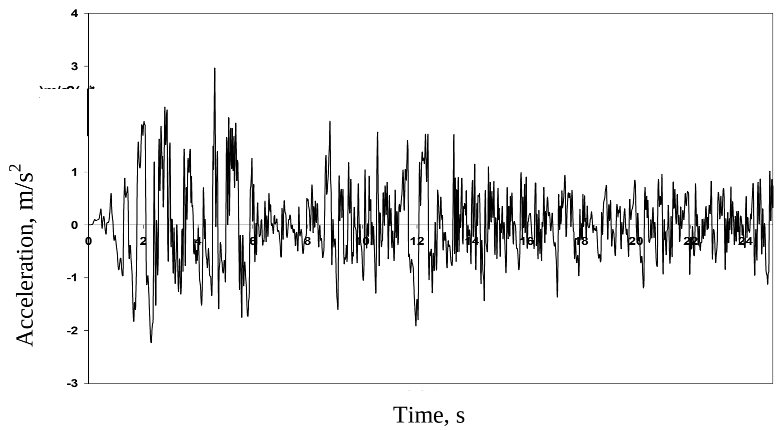

Fig. 10. Free field acceleration due to El Centro excitation for non-linear system using FLAC3D

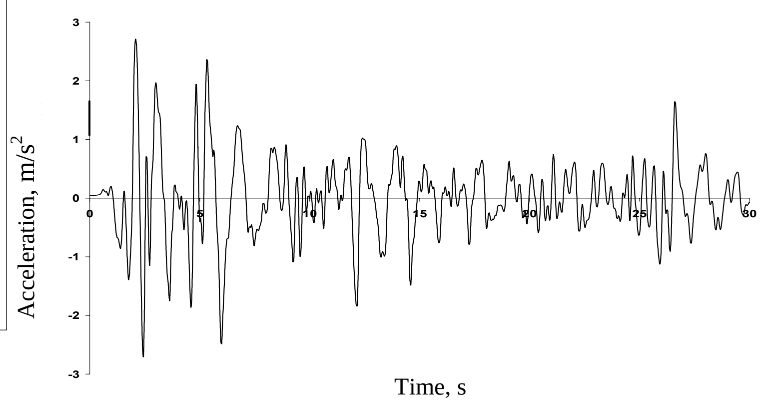

Fig. 11. Free field acceleration due to El Centro excitation for non-linear system using SHAKE91

selected as the control free-field motions to represent the different excitation parameters including: acceleration/velocity ratios of the earthquakes, peak ground acceleration, frequency content and duration of the excitation. For a given excitation, appropriate site dynamic parameters are chosen to be compatible with the predominant frequency of excitation

Table 1. Soil Dynamic Parameters

Soil Parameters / Earthquake	Density	ϕ^o	c (kPa)	ν	Predominant Frequency	ψ^o	G_{max} (Mpa)	V_s (m/s)
El Centro	1800	30	1	0.30	1.8	5	30.2	129.6
Northridge	2000	30	1	0.30	3	5	93.3	216

leading enforcement to the inelastic behavior of the soil (Table 1). For each soil type, the seismic response of the soil-structure system is determined assuming fully normal contact between the basement wall and surrounding soil. The calculated response time histories of the structure subjected to El Centro and Northridge ground motions for the roof and base displacements are shown in Figs. 12 to 15. As it can be noted from Figs. 12 to 15 the primary and secondary soil non-linearities resulted in changes in the displacement of the structure.

Figs. 16 and 17 show the calculated maximum displacement of the structure at the floors accounting for non-linear *SSI*, where it can be also compared with the corresponding values for the linear *SSI* case. As it can be noted in this case, the effect of soil non-linearity is to decrease the floors displacements compared with the linear *SSI* case mainly because of primary soil non-linearity in the free-field analysis. However, when it comes to the secondary non-linearity in the kinematic and inertial interaction the effect of soil hysteretic behavior is to increase the relative displacements.

The normal stresses of the soil-structure interface at the base level are computed using 1994 Northridge ground motion. The results assuming linear and non-linear behavior of the supporting soil are shown in Figs. 18 and 19. It is interesting to note that as the supporting soil undergoes into the non-linear behavior zone, the normal stresses at the base increase. However, this effect strongly depends on the excitation parameters. For linear and non-linear soil behavior, the calculated shear stresses at the base level (soil-structure interface) have also been plotted in Figs. 20 and 21. As it can be noted the soil non-linearities resulted in an increase in the shear stresses of the structure at the base.

The response amplitude spectra of the structure's accelerations at the bedrock, base level and roof level are shown in Figs. 22 and 23 corresponding to linear and non-linear soil behaviors, respectively. It can be seen from figures that, in general the frequency content of the free-field motion is almost similar to the frequency content of applied ground motion for the linear soil behavior case. However, for the non-linear case the frequency contents of the responses at the base and the roof are not comparable with the frequency content of the bedrock input motion. These results indicate the importance of the non-linearities of the supporting soil on the dynamic soil-structure interaction phenomenon.

CONCLUSIONS

A simple algorithm to define the soil hysteretic loops during loading-reloading phase of excitation is implemented into the direct soil-structure analysis method. The elastic behavior of supporting soil in the soil-structure system was assumed to show the hysteretic characteristics based on the hyperbolic model for stress-strain relationships, either in free-field analysis or in inertial analysis. In the plastic zone the Mohr-Coulomb failure constitutive model was adopted. The seismic response of a practical shear building with underground story supporting on shallow foundation subjected to different earthquake excitations were determined assuming the linear and non-linear soil-structure interaction. The following conclusions are drawn:

- the soil primary non-linearity in the free-field response attenuates the bedrock input motion. This phenomenon was taken into account using a fully non-linear time history analysis rather than the commonly used equivalent linear method.
- the secondary soil non-linearity increase the lateral displacements of the structure; however, it may result in an increase or decrease in the base forces compared to those of the linear soil model case, depending on the type of structure, frequency of the base input motion. It also alters the frequency content of the response, especially for the interface forces. Due to softening phenomenon occurred from non-linear deformations during an earthquake, the normal forces existing at the soil-structure interface may increase and then this should be considered in the design of the underground stories.

ACKNOWLEDGEMENT

This research was funded by Isfahan University of Technology. Their support is greatly appreciated.

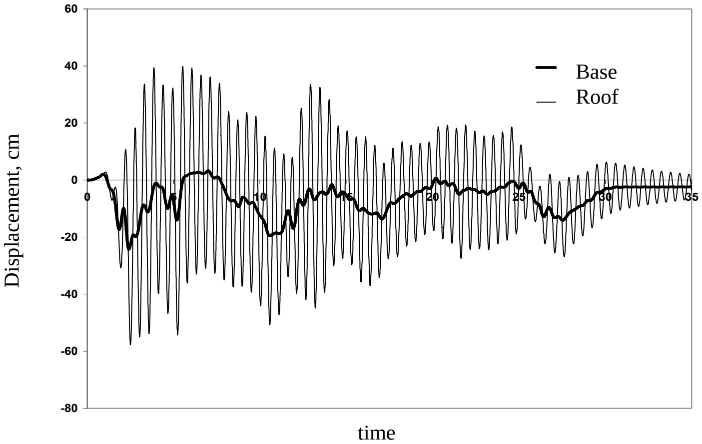

Fig. 12. Displacement time histories of the structure's base and roof subjected to EL Centro for soil linear behavior

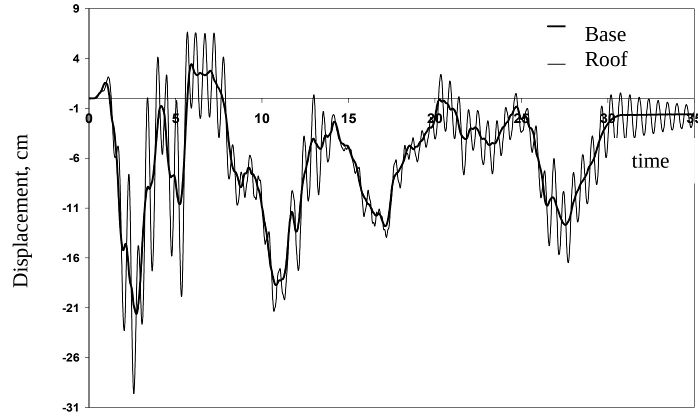

Figure 13. Displacement time histories of the structure's base and roof subjected to EL Centro for soil non- linear behavior

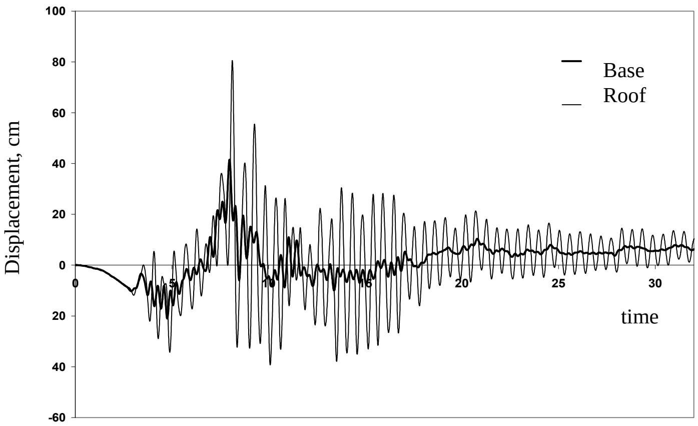

Fig. 14. Displacement time histories of the structure's base and roof subjected to Northridge for soil linear behavior

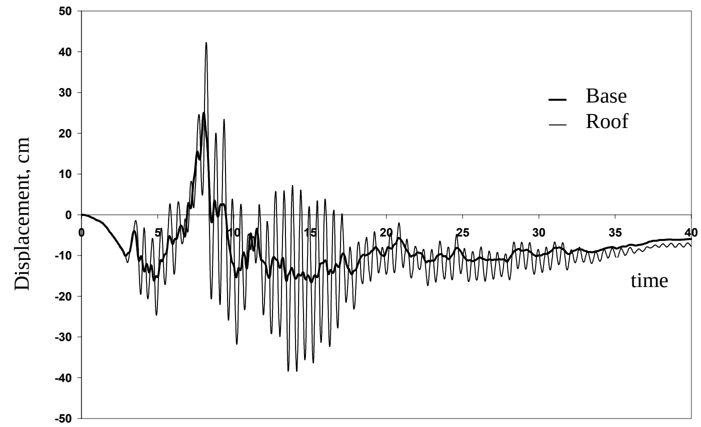

Figure 15. Displacement time histories of the structure's base and roof subjected to Northridge for soil non- linear behavior

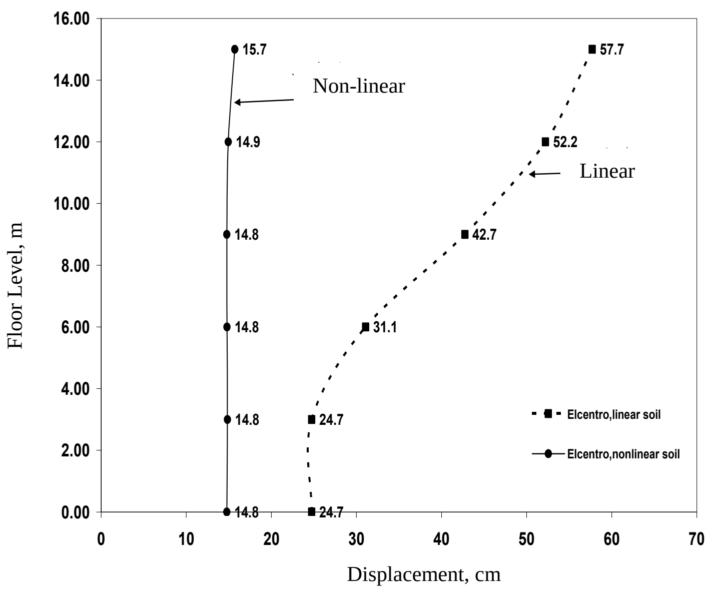

Fig. 16. Variation of maximum displacements of the floors due to El Centro for soil linear and nonlinear behavior

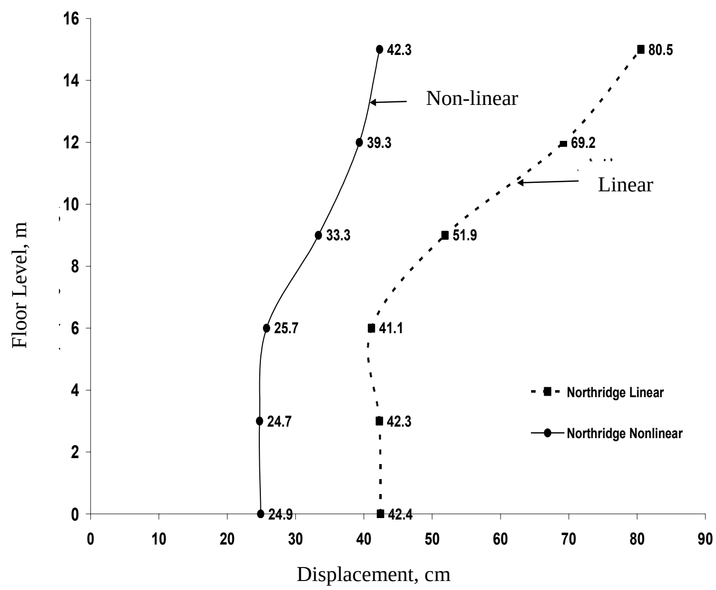

Fig. 17. Variation of maximum displacements of the floors due to Northridge for soil linear and nonlinear behavior

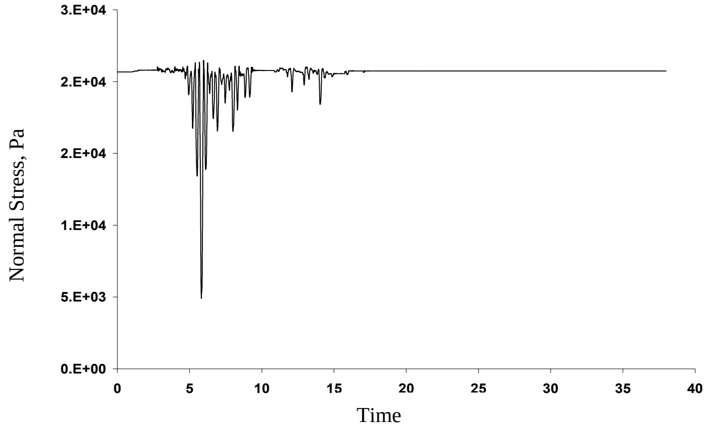

Fig. 18. The time history of the normal stress at the base of the structure subjected to Northridge for soil linear behavior

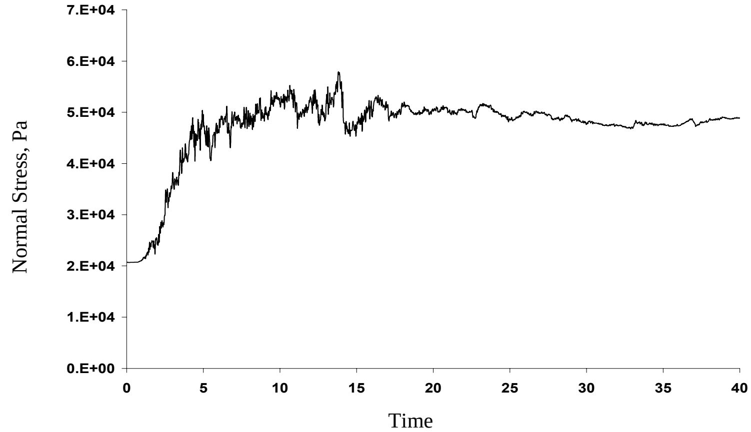

Fig. 19. The time history of the normal stress at the base of the structure subjected to Northridge for soil non-linear behavior

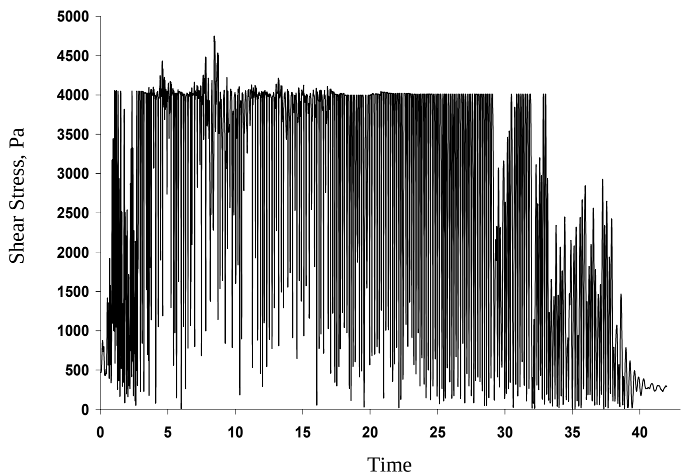

Fig. 20. The time history of the shear stress at the base of the structure subjected to Northridge for soil linear behavior

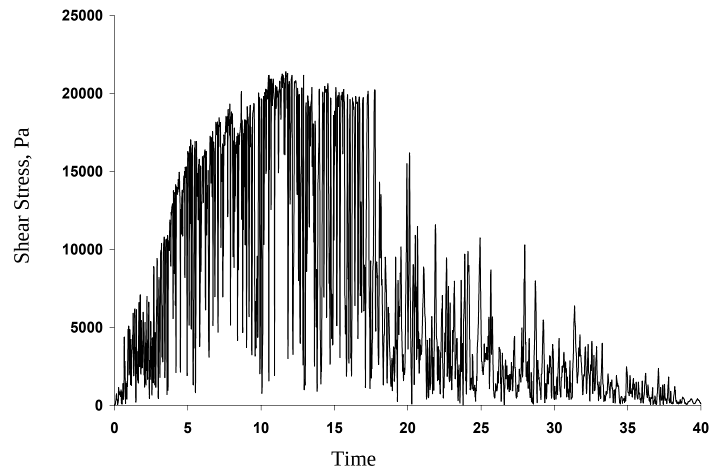

Fig. 21. The time history of the shear stress at the base of the structure subjected to Northridge for soil non-linear behavior

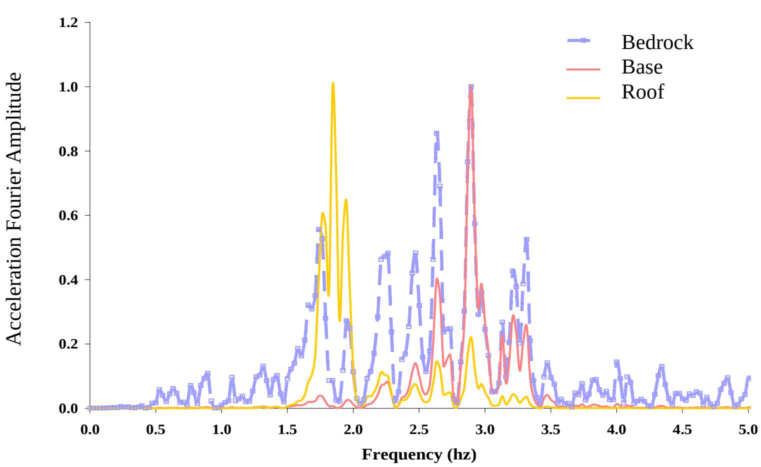

Fig. 22. Displacement time histories of the structure's base and roof subjected to Northridge for soil linear behavior

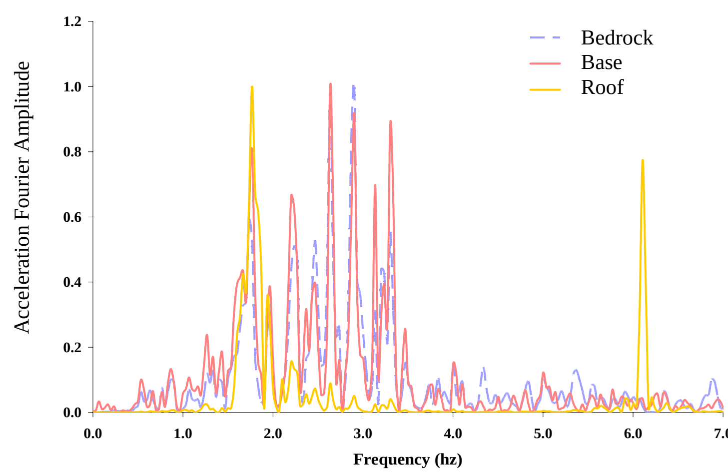

Fig. 23. Displacement time histories of the structure's base and roof subjected to Northridge for soil non- linear behavior

REFERENCES

"FLAC 3D's Manual" [1996], *Itasca Consulting group, Inc.*, Minneapolis, Minnesota, USA.

Ishihara, K. [1996], "Soil Behavior in Earthquake Geotechnics", *Department of Civil Engineering Science University of Tokyo*.

Finn, W. D. and Lee, W. [1977], "An Effective Stress Model For Liquefaction", *ASCE Journal, Geotechnical Engineering Division*, GT.6, pp. 517-533.

Prakash, S. [1981], "*Soil Dynamics".* McGraw-Hill, Inc.